

Structure and Physical Properties of Trigonal Monopyramidal Iron(II), Cobalt(II), Nickel(II), and Zinc(II) Complexes

Manabendra Ray,^{†,‡} Brian S. Hammes,[†] Glenn P. A. Yap,[§] Arnold L. Rheingold,[§] and A. S. Borovik^{*,†,‡}

Departments of Chemistry, Kansas State University, Manhattan, Kansas 66506, and University of Delaware, Newark, Delaware 19716

Received July 3, 1997

A series of trigonal monopyramidal complexes of the tripodal ligand tris(*N*-*tert*-butylcarbamoyl)methylaminato, $[1^{Bu}]^{3-}$, have been synthesized and characterized. The structures of $[Co1^{Bu}]^{-}$, $[Zn1^{Bu}]^{-}$, and $[Ni1^{Bu}]^{-}$ confirm that trigonal monopyramidal coordination geometry occurs in these complexes where the three amidate nitrogens are arranged in the trigonal plane and the amine nitrogen is bonded apically to the metal ions. The solid-state structures of $[Co1^{Bu}]^{-}$, $[Zn1^{Bu}]^{-}$, and $[Ni1^{Bu}]^{-}$ are nearly identical indicating that the trigonal ligand $[1^{Bu}]^{3-}$ enforces the trigonal monopyramidal structure in these metal ions. Crystal data: $K[Co1^{Bu}] \cdot 0.5DMF$ crystallizes in the monoclinic space group $C2/c$, with cell dimensions $a = 18.844(4)$ Å, $b = 9.809(3)$ Å, $c = 28.715(13)$ Å, $\beta = 102.70^\circ$, and $Z = 8$; $(NEt_4)[Zn1^{Bu}] \cdot THF$ crystallizes in the monoclinic space group $P2_1/c$, with cell dimensions $a = 13.244(3)$ Å, $b = 11.285(5)$ Å, $c = 25.625(3)$ Å, $\beta = 104.45(1)^\circ$, and $Z = 4$. The 1H NMR spectrum of the diamagnetic $[Zn1^{Bu}]^{-}$ also suggests that the complex retains its C_3 symmetry in solution. Room-temperature magnetic susceptibility measurements show that $[Fe1^{Bu}]^{-}$, $[Co1^{Bu}]^{-}$, and $[Ni1^{Bu}]^{-}$ are high spin. The cyclic voltammetry of $[Co1^{Bu}]^{-}$ and $[Ni1^{Bu}]^{-}$ at a glassy carbon surface and at a scan rate of 100 mV s^{-1} shows quasi-reversible one electron oxidation at $E_{1/2} = 0.77$ ($\Delta E_p = 93 \text{ mV}$, $i_{pa} i_{pc}^{-1} = 0.69$) and 0.56 ($\Delta E_p = 75 \text{ mV}$, $i_{pa} i_{pc}^{-1} = 0.79$) V versus SCE, respectively. However, at slower scan rates these redox processes become irreversible and attempts to isolate the oxidized products at room temperature were unsuccessful. The chemical oxidation of $[Ni1^{Bu}]^{-}$ with $[Fe(bpy)_3]^{3+}$ in 1:1 propionitrile–DMF mixture at -75°C generated a EPR-active species (77 K , $g_1 = 2.29$, $g_2 = 2.16$, $g_3 = 2.03$, $a_3 = 20 \text{ G}$) assigned to a Ni(III) complex with rhombic symmetry. $[Fe1^{Bu}]^{-}$ shows one irreversible oxidation ($E_{p,a} = 0.05 \text{ V}$ versus SCE) under the same conditions. These results are consistent with $[1^{Bu}]^{3-}$ being able to stabilize trigonal monopyramidal complexes of low-valent metal ions.

Introduction

Trigonal monopyramidal coordination geometry is uncommon for transition metal ions. Structural examples of TMP complexes are dominated by those containing d^{10} metals which, lacking crystal field stabilization energy, can easily be distorted from the more favored tetrahedral geometry and, being coordinatively saturated, are unlikely to form five-coordinate trigonal bipyramidal complexes.¹ Tripodal ligands, such as $(Ph_2PCH_2CH_2)_3N$ and $(PyCH_2)_3N$, are the most successful ligand systems for the isolation of these TMP complexes.^{1a,2} By contrast, there are few ligand systems that can support TMP coordination around metal ions with nonspherical distribution of electrons.³

Schrock has recently shown⁴ that tris(amido) amine ligands⁵ $[(XNCH_2CH_2)_3N]^{3-}$ ($X = R_3Si$ or C_6F_5) can form TMP complexes with trivalent first-row transition metal ions, and structural data for V(III)–TMP complexes have been reported. The bulky R groups ($R = \text{alkyl}$ or aryl) can partially shield the vacant coordination site which limits the binding of additional ligands to the coordinatively unsaturated metal ions. However, this shielding is incomplete and several trigonal bipyramidal complexes of these $[(XNCH_2CH_2)_3N]^{3-}$ have been isolated. We have been investigating the coordination chemistry of tripodal ligands derived from nitrilotriacetamide, $[(RNHC(O)CH_2)_3N]$.^{6,7} In particular, the deprotonated form of tris(*N*-*tert*-butylcar-

* To whom correspondence should be addressed.

[†] Kansas State University.

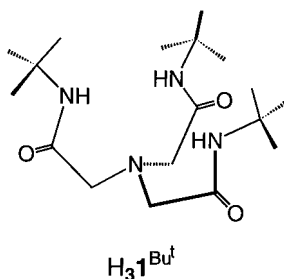
[‡] Current address: Department of Chemistry, University of Kansas, Lawrence, KS 66045.

[§] University of Delaware.

- (1) (a) Mealli, C.; Sacconi, L. *J. Chem. Soc., Chem. Commun.* **1973**, 886. (b) Karlin, K. D.; Dahlstrom, P. L.; Stanford, M. L.; Zubieta, J. *J. Chem. Soc., Chem. Commun.* **1979**, 465. (c) Karlin, K. D.; Dahlstrom, P. L.; Hyde, J. R.; Zubieta, J. *J. Chem. Soc., Chem. Commun.* **1980**, 906. (d) Chuang, C.; Lim, K.; Chen, K.; Zubieta, J.; Canary, J. W. *Inorg. Chem.* **1995**, *34*, 2562. (e) de Mendoza, J.; Mesa, E.; Robdriguez-Ubis, J.-C.; Vázquez, P.; Vögtle, F.; Windscheif, P.-M.; Rissanen, K.; Lehn, J.-M.; Liliensbaum, D.; Ziessel R. *Angew. Chem., Int. Ed. Engl.* **1991**, *30*, 1331. (f) Pinkas, J.; Wang, T.; Jacobson, R. A.; Verkade, J. G. *Inorg. Chem.* **1994**, *33*, 4202.
- (2) Mealli, C.; Ghilardi, C. A.; Orlandini, A. *Coord. Chem. Rev.* **1992**, *120*, 361 and references therein.

- (3) (a) Sacconi, L.; Orlandini, A.; Midollini, S. *Inorg. Chem.* **1974**, *13*, 2850. (b) Mani, F.; Mealli, C. *Inorg. Chim. Acta* **1981**, *54*, L77. (c) Dietrich-Buchecker, C. O.; Guilhem, J.; Kern, J.-M.; Pscard, C.; Sauvage, J.-P. *Inorg. Chem.* **1994**, *33*, 3498.
- (4) (a) Cummins, C. C.; Lee, J.; Schrock, R. R.; Davis, W. D. *Angew. Chem., Int. Ed. Engl.* **1992**, *31*, 1501. (b) Cummins, C. C.; Schrock, R. R.; Davis, W. D. *Inorg. Chem.* **1994**, *33*, 1448 and references therein. (c) Schrock, R. R. *Acc. Chem. Res.* **1997**, *30*, 9.
- (5) Plass, W.; Verkade, J. G. *J. Am. Chem. Soc.* **1992**, *114*, 2275.
- (6) (a) Ray, M.; Yap, G. P. A.; Rheingold, A.; Borovik, A. S. *J. Chem. Soc., Chem. Commun.* **1995**, 1777. (b) Ray, M.; Golombek, A. P.; Hendrich, M. P.; Young, V. G., Jr.; Borovik, A. S. *J. Am. Chem. Soc.* **1996**, *118*, 6084. (c) Hammes, B. S.; Ramos-Maldonado, D.; Yap, G. P. A.; Liable-Sands, L.; Rheingold, A. L.; Young, V. G., Jr.; Borovik, A. S. *Inorg. Chem.* **1997**, *36*, 3210.
- (7) The lead complex of nitrilotriacetamide has been reported: Smith, D. A.; Sucheck, S.; Pinkerton, A. A. *J. Chem. Soc., Chem. Commun.* **1992**, 367.

bamoyl)methyl)amine ($[(\text{Bu}^t\text{NC}(\text{O})\text{CH}_2)_3\text{N}]^{3-}$, $[\mathbf{1}^{\text{Bu}^t}]^{3-}$) can



provide a constrained coordination environment around the bound metal ion which permits the isolation of TMP complexes. Reported herein are the synthesis and structural and physical properties for the TMP complexes of Fe(II), Co(II), Ni(II), and Zn(II) with $[\mathbf{1}^{\text{Bu}^t}]^{3-}$.

Experimental Section

All reagents and solvents were purchased from commercial sources and used as received unless otherwise noted. The metal precursor $[\text{Co}(\text{DMSO})_6](\text{ClO}_4)_2$ ⁸ and $(\text{NEt}_4)[\text{Ni}\mathbf{1}^{\text{Bu}^t}]$ ^{6a} were prepared by following procedures previously reported. (*CAUTION! Perchlorate salts can be explosive.*)

Tris((*N*-*tert*-butylcarbamoyl)methyl)amine ($\text{H}_3\mathbf{1}^{\text{Bu}^t}$). *tert*-Butylamine (8.40 g, 115 mmol) was added dropwise to a slurry of nitrilotriacetic acid (5.70 g, 29.8 mmol) in 40 mL of distilled pyridine and stirred for 1 h. After heating this mixture to 100 °C, triphenyl phosphite (27.0 g, 87.1 mmol) was added dropwise. The reaction mixture was stirred at 110 °C for 12 h, after which the pyridine was removed under reduced pressure and the resulting oil was dissolved in chloroform. The chloroform solution was washed three times each with H₂O, saturated sodium bicarbonate, and again with H₂O, and the organic layer was dried over anhydrous MgSO₄. Volatiles were removed under reduced pressure to yield a white powder that was washed several times with diethyl ether and dried at 50 °C under reduced pressure for 12 h to afford 3.5 g (33%) of the $\text{H}_3\mathbf{1}^{\text{Bu}^t}$: ¹H NMR (CDCl₃) δ 7.11 (s, 3 H, NH), 3.16 (s, 6 H, $-\text{CH}_2-$), 1.37 (s, 27 H, $-\text{CH}_3$); MH^+ *m/e* 357 (Cl, isobutane); FTIR (KBr, cm⁻¹) ν (NH) 3342 (s), 3279 (s), 3222 (sh), ν (CO) 1681 (s), 1666 (s), 1646 (s); mp 172–180 °C.

Potassium [Tris((*N*-*tert*-butylcarbamoyl)methyl)aminato]ferrate(II), $\text{K}[\text{Fe}\mathbf{1}^{\text{Bu}^t}]$. A solution of $\text{H}_3\mathbf{1}^{\text{Bu}^t}$ (0.20 g, 0.56 mmol) in 10 mL of anhydrous DMF was treated with solid KH (0.070 g, 1.7 mmol) under an Ar atmosphere. After gas evolution ceased, solid Fe(acetate)₂ (0.10 g, 0.57 mmol) was added slowly. The resulting solution was stirred for 1 h and filtered to remove a small amount of insoluble material. The filtrate was concentrated under reduced pressure to a volume of 4 mL, and diethyl ether was added slowly. Over a 2 day period $\text{K}[\text{Fe}\mathbf{1}^{\text{Bu}^t}]$ crystallized as white needles, which were filtered out and dried under reduced pressure (0.11 g, 37%). Anal. Calcd (found) for $\text{K}[\text{Fe}(\text{L}^{\text{Bu}^t})]\cdot\text{DMF}$, C₂₁H₄₀FeKN₅O₄: C, 48.36 (47.68); H, 7.73 (7.19); N, 13.43 (12.66); Fe, 10.71 (11.00); K, 7.50 (7.75). FTIR (Nujol, cm⁻¹): ν (CO) 1668 (DMF, s), 1602, 1576, 1567 (amide, s). λ_{max} (DMF): 314 (sh), 395 (sh). ¹H NMR (DMSO-*d*₆): δ 2.75 (s), 2.92 (s), 7.97 (s), 36.84 (br), -61.78 (br).

Potassium [tris((*N*-*tert*-butylcarbamoyl)methyl)aminato]cobaltate(II), $\text{K}[\text{Co}\mathbf{1}^{\text{Bu}^t}]$, was prepared as described for $\text{K}[\text{Fe}\mathbf{1}^{\text{Bu}^t}]$, using $[\text{Co}(\text{DMSO})_6](\text{ClO}_4)_2$ as the cobalt precursor (57% yield), and crystallized by vapor diffusion of diethyl ether into a DMF solution of $\text{K}[\text{Co}\mathbf{1}^{\text{Bu}^t}]$. Anal. Calcd (found) for $\text{K}[\text{Co}\mathbf{1}^{\text{Bu}^t}]\cdot 0.5\text{DMF}$, [C₁₈H₃₃CoKN₄O₃] $\cdot 0.5\text{C}_3\text{H}_7\text{NO}$: C, 47.98 (47.91); H, 7.53 (7.49); N, 12.91 (12.92). IR (Nujol, cm⁻¹): ν (CO) 1673 (DMF, s), 1603, 1577, 1568 (amide, s). λ_{max} (DMF, ϵ , M⁻¹ cm⁻¹): 414 (20), 576 (145), 602(130), 659 (sh). X-band EPR: powder, 77 K, $g = 4.18$; DMF, 77 K, $g = 4.10$. ¹H NMR (DMSO-*d*₆): δ 2.75 (s), 2.92 (s), 7.97 (s), 23.5 (br), 78.5 (br).

Tetraethylammonium [Tris((*N*-*tert*-butylcarbamoyl)methyl)aminato]zincate(II), $(\text{NEt}_4)[\text{Zn}\mathbf{1}^{\text{Bu}^t}]$. The potassium salt of this complex was prepared by following the same method as used for the other complexes with ZnCl₂ as the metal precursor. The complex was then treated with NEt₄Cl in DMF (yield: 65%) and crystallized by vapor diffusion of diethyl ether into a THF solution of $(\text{NEt}_4)[\text{Zn}\mathbf{1}^{\text{Bu}^t}]$. Anal. Calcd (found) for $(\text{NEt}_4)[\text{Zn}\mathbf{1}^{\text{Bu}^t}]$, C₂₆H₅₃N₅O₃Zn: C, 56.87 (56.69); H, 9.73 (9.53); N, 12.75 (12.64). FTIR (Nujol, cm⁻¹): ν (CO) 1603, 1582 (amide, s). ¹H NMR (CD₃CN): δ 1.20 (t, 12 H, N(CH₂CH₃)₄⁺), 3.16 (q, 8 H, N(CH₂CH₃)₄⁺), 1.34 (s, 27 H, $-\text{CH}_3$), 2.85 (s, 6 H, $-\text{CH}_2-$).

Physical Methods. Elemental analyses were performed by Desert Analytics (Tucson, AZ). All samples used for elemental analyses were dried under vacuum before shipment. The presence of solvates was corroborated by FTIR and ¹H NMR spectroscopy. Electronic spectra were recorded with a SLM-Aminco 3000 diode array spectrophotometer. ¹H NMR spectra were recorded on a Varian Unity Plus 400 MHz spectrometer equipped with a Sun workstation. Chemical shifts are reported in ppm relative to an internal standard of TMS. FTIR spectra were recorded on a Mattson Sirius 100 FTIR spectrometer (with an 4326 upgrade) and are reported in wavenumbers. Fast atom bombardment mass spectra (FAB-MS) were recorded on a Hewlett-Packard 5989 A spectrometer. Room-temperature magnetic susceptibility measurements of the solid samples were obtained using a MSB-1 magnetic susceptibility balance manufactured by Johnson Matthey. Solution magnetic moments were measured by following Evan's method.⁹ Diamagnetic corrections were taken from those reported by O'Connor.¹⁰ X-band EPR spectra were collected using a Bruker TE₁₀₂ cavity and a Bruker 200D-SRC control console (which housed a Bruker ER022 signal channel, a Bruker ER031 field controller, and a Bruker ER001 time base oscilloscope). The console was interfaced to a Bruker ER040 XR microwave bridge and a Varian V3603 magnet (powered by Varian model 907015-03 power supply and a Varian V-FR2503 Fieldial magnetic field regulator). All *g*-values reported are referenced versus DPPH. A quartz liquid nitrogen finger-dewar (Willmad Glass) was used to record spectra at 77K. Extended Hückel calculations were done on a Power Macintosh 7600 with software provided by CAChe Scientific (version 3.8).

Cyclic voltammetric experiments were conducted using a BAS CV 50W (Bioanalytical Systems Inc., West Lafayette, IN) voltammetric analyzer. All experiments were done under argon at ambient temperature in solutions with 0.1 M tetrabutylammonium hexafluorophosphate as the supporting electrolyte. Acetonitrile and anhydrous DMF were obtained from Burdick-Jackson Laboratory and Aldrich Chemical Co., respectively, and used without further purification. Cyclic voltammograms (CV) were obtained using a three-component system consisting of a glassy-carbon working electrode, a platinum wire auxiliary electrode, and a glass encased nonaqueous silver–silver nitrate reference electrode containing a Vycor plug to separate it from the bulk solution. A ferrocene/ferrocene couple was used to monitor the reference electrode and was observed at 0.46 V with $\Delta E_p = 0.070$ V and $i_{pc}i_{pa}^{-1} \cong 1.0$ in DMF and 0.40 V with $\Delta E_p = 0.065$ V and $i_{pc}i_{pa}^{-1} \cong 1.0$ in CH₃CN. IR compensation was achieved before each CV was recorded. Potentials are reported vs the saturated calomel couple. Controlled potential coulometry was performed with a PAR 175 digital coulometer using a system composed of a platinum mesh working electrode, a platinum mesh auxiliary electrode encased in a glass tube with supporting electrolyte solution and separated from the bulk solution by a medium porous-glass frit, and the same silver–silver nitrate reference electrode used for the CV experiments.

Crystallographic Structural Determination. Crystal, data collection, and refinement parameters for $\text{K}[\text{Co}\mathbf{1}^{\text{Bu}^t}]\cdot 0.5\text{DMF}$ and $(\text{NEt}_4)[\text{Zn}\mathbf{1}^{\text{Bu}^t}]\cdot\text{THF}$ are given in Table 1. The systematic absences in the diffraction data are consistent with the space groups *Cc* or *C2/c* for $\text{K}[\text{Co}\mathbf{1}^{\text{Bu}^t}]\cdot 0.5\text{DMF}$ and uniquely consistent with the reported space group for $(\text{NEt}_4)[\text{Zn}\mathbf{1}^{\text{Bu}^t}]\cdot\text{THF}$. The *E*-statistics and the value of *Z* indicated the centrosymmetric space group for $\text{K}[\text{Co}\mathbf{1}^{\text{Bu}^t}]\cdot 0.5\text{DMF}$ which was verified by the chemically reasonable and computationally stable

(8) Cotton, F. A.; Francis, F. J. *Am. Chem. Soc.* **1960**, 82, 2986.

(9) (a) Evans, D. F. *J. Chem. Soc.* **1959**, 2003. (b) Sur, S. K. *J. Magn. Reson.* **1989**, 82, 169.

(10) O'Connor, C. J. *Prog. Inorg. Chem.* **1992**, 29, 203.

Table 1. Summary of Crystallographic Data and Parameters for the $[\text{CoI}^{\text{Bu}}]^-$ and $[\text{ZnI}^{\text{Bu}}]^-$ Complexes

	$\text{K}[\text{CoI}^{\text{Bu}}] \cdot 0.5\text{DMF}$	$(\text{NEt}_4)[\text{ZnI}^{\text{Bu}}] \cdot \text{THF}$
molecular formula	$\text{C}_{19.5}\text{H}_{36.5}\text{CoKN}_{4.5}\text{O}_{3.5}$	$\text{C}_{30}\text{H}_{61}\text{N}_5\text{O}_4\text{Zn}$
fw	488.06	621.21
temp ($^\circ\text{C}$)	25(2)	23(2)
cryst system	monoclinic	monoclinic
space group	$C2/c$	$P2_1/c$
cell constants		
a (\AA)	18.844(4)	13.244(3)
b (\AA)	9.809(3)	11.285(5)
c (\AA)	28.715(13)	25.625(3)
α (deg)	90	90
β (deg)	102.70	104.45(1)
γ (deg)	90	90
Z	8	4
V (\AA^3)	5178(3)	3709(1)
abs coeff, μ_{calc} (cm^{-1})	8.51	6.98
δ_{calc} (g/cm^3)	1.271	1.113
$F(000)$	2072	1352
cryst dimens (mm)	$0.30 \times 0.20 \times 0.10$	$0.30 \times 0.30 \times 0.30$
radiation	Mo $K\alpha$	Mo $K\alpha$
	$(\lambda = 0.71073 \text{ \AA})$	$(\lambda = 0.71073 \text{ \AA})$
h, k, l ranges colld	$-23 \rightarrow 22, 0 \rightarrow 12, 0 \rightarrow 35$	$-1 \rightarrow 13, -14 \rightarrow 11, -26 \rightarrow 26$
θ range (deg)	$2.22 - 26.00$	$2.41 - 30.07$
no. of reflns colld	5178	5508
no. of indepdt reflns	5068	4225
no. of params	281	361
data/param ratio	18.0	11.7
refinement method	full-matrix least-squares on F^2	full-matrix least-squares on F^2
$R(F)^a$	0.0347	0.0440
$R_w(F^2)^b$	0.0634	0.0949
GOF ^c	0.764	1.018
largest diff peak and hole ($e/\text{\AA}^3$)	0.253 and -0.377	0.228 and -0.274

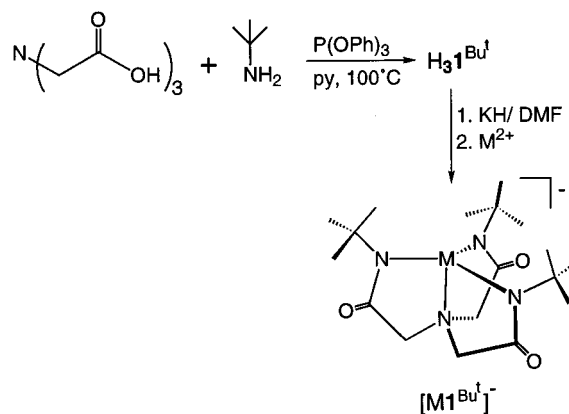
^a $R = [\sum |\Delta F| / \sum |F_o|]$. ^b $R_w = [\sum w(\Delta F)^2 / \sum wF_o^2]$. ^c Goodness of fit on F^2 .

results of refinement. The structures were solved using direct methods, completed by subsequent difference Fourier syntheses, and refined by full-matrix least-squares procedures. Semiempirical ellipsoid absorption corrections were applied to the data for $\text{K}[\text{CoI}^{\text{Bu}}] \cdot 0.5\text{DMF}$ but were not required for $(\text{NEt}_4)[\text{ZnI}^{\text{Bu}}] \cdot \text{THF}$ because there was less than 10% variation in the integrated ψ -scan intensity data. The asymmetric unit of $\text{K}[\text{CoI}^{\text{Bu}}] \cdot 0.5\text{DMF}$ contains half of a molecule of DMF; the nitrogen and oxygen atoms are on a 2-fold axis, and the carbon atoms are equally disordered over the 2-fold axis. The asymmetric unit of $(\text{NEt}_4)[\text{ZnI}^{\text{Bu}}] \cdot \text{THF}$ contains a molecule of THF. All non-hydrogen atoms were refined with anisotropic displacement coefficients, and hydrogen atoms were treated as idealized contributions. All software and sources of the scattering factors are contained in the SHELXTL (5.3) program library (G. Sheldrick, Siemens XRD, Madison, WI).

Results and Discussion

Design Considerations and Syntheses. Isolation of TMP complexes is often difficult because (1) four-coordinate transition metal ions prefer to have either tetrahedral or square planar coordination geometries and (2) TMP coordination renders the complexes coordinatively unsaturated (for non- d^{10} metal ion complexes) which causes nearly all complexes to readily bind additional ligands. $[\text{I}^{\text{Bu}}]^{3-}$ was designed to overcome these problems. The ligand contains three deprotonated amide moieties (amidates) and one tertiary amine. Margerum¹¹ and Collins¹² have shown that amidates are strong σ -donors which bind to metal ions via coordination of the nitrogen atoms. We

Scheme 1

**Table 2.** Selected Bond Distances and Angles for the $[\text{CoI}^{\text{Bu}}]^-$, $[\text{NiI}^{\text{Bu}}]^-$, and $[\text{ZnI}^{\text{Bu}}]^-$ Complexes

dist (\AA) or angle (deg)	$[\text{CoI}^{\text{Bu}}]^-$	$[\text{NiI}^{\text{Bu}}]^-$	$[\text{ZnI}^{\text{Bu}}]^-$
M–N(1)	1.972(2)	1.975(5)	1.978(4)
M–N(2)	1.970(2)	1.981(5)	1.988(3)
M–N(3)	1.974(2)	1.960(5)	1.991(3)
M–N(4)	2.050(2)	2.003(5)	2.071(3)
N(1)–M–N(2)	116.81(9)	114.3(2)	121.1(2)
N(1)–M–N(3)	119.44(9)	125.0(2)	120.3(2)
N(2)–M–N(3)	120.91(10)	119.2(2)	117.18(14)
N(1)–M–N(4)	84.57(10)	86.2(2)	86.02(14)
N(2)–M–N(4)	84.42(9)	85.6(2)	85.73(14)
N(3)–M–N(4)	84.16(8)	85.8(2)	86.15(13)
$d[\text{M} - \text{N}_{\text{amid}}]^a$	0.19	0.14	0.14

^a Displacement of metal ion from the plane formed by N(1), N(2), and N(3).

reasoned that this type of donor atom should be sufficient to stabilize the coordinatively unsaturated metal ions in the TMP geometry. Moreover, upon metal ion binding, three five-membered chelate rings are formed that are relatively rigid to enforce trigonal coordination of the amidate nitrogens and prevent distortion toward a tetrahedral geometry. These nitrogen atoms also contain appended *tert*-butyl groups that should provide enough steric hindrance around the vacant coordination sites on the TMP complex to allow the isolation of coordinatively unsaturated metal complexes.

$\text{H}_3\text{I}^{\text{Bu}}$ was synthesized by a one-step route from *tert*-butylamine and nitrilotriacetic acid in pyridine using triphenyl phosphite as the dehydration agent (Scheme 1). Deprotonation of $\text{H}_3\text{I}^{\text{Bu}}$ with 3 equiv of KH in DMF yielded $[\text{I}^{\text{Bu}}]^{3-}$, which reacts rapidly with divalent metal ions as is apparent by the immediate color change observed upon addition of Co(II) and Ni(II) ions. $\text{K}[\text{CoI}^{\text{Bu}}]$ and $\text{K}[\text{NiI}^{\text{Bu}}]$ have relatively low solubility in DMF and can be precipitated from concentrated solution during workup.

Solid-State Structures of the Complexes. Single-crystal X-ray diffraction studies on $\text{K}[\text{CoI}^{\text{Bu}}]$ and $(\text{NEt}_4)[\text{ZnI}^{\text{Bu}}]$ confirm the TMP coordination geometry in these complexes. Selected distances and angles for structures of these complexes are shown in Table 2, and Figure 1 contains the thermal ellipsoid diagrams for $[\text{CoI}^{\text{Bu}}]^-$ and $[\text{ZnI}^{\text{Bu}}]^-$. Additional structural parameters are provided in the Supporting Information. The molecular structure of $[\text{NiI}^{\text{Bu}}]^-$ has been reported and shown to be TMP geometry.^{6a} Its structure will be discussed only in relation to that of the other complexes. $\text{K}[\text{FeI}^{\text{Bu}}]$ is extremely air-sensitive, which hindered its molecular structure determination by X-ray diffraction. However, we have reported recently

(11) Margerum, D. W. *Pure Appl. Chem.* **1983**, *55*, 23.

(12) Collins, T. J. *Acc. Chem. Res.* **1994**, *27*, 279.

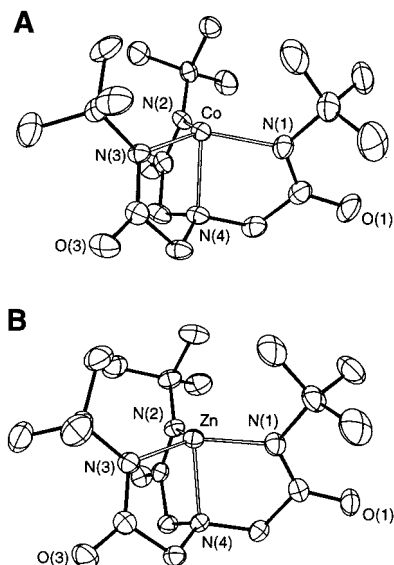


Figure 1. Thermal ellipsoid diagrams of $[\text{Co1}^{\text{Bu}}]^-$ (A) and $[\text{Zn1}^{\text{Bu}}]^-$ (B). The ellipsoids are drawn at the 40% probability level, and hydrogens are removed for clarity.

the molecular structure of a related complex, $\text{K}[\text{Fe1}^{\text{Pr}}]$ (Pr = appended isopropyl groups), that contains a TMP arrangement of atoms about the Fe(II) ion.^{6b}

The molecular structures of $[\text{Co1}^{\text{Bu}}]^-$, $[\text{Zn1}^{\text{Bu}}]^-$, and $[\text{Ni1}^{\text{Bu}}]^-$ show that the three amidate nitrogen donors of $[\text{1}^{\text{Bu}}]^{3-}$ are coordinated in the trigonal plane. The average $\text{N}_{\text{amid}}-\text{M}-\text{N}_{\text{amid}}$ angle for the complexes are statistically the same, ranging from $119.05(6)^\circ$ in $[\text{Co1}^{\text{Bu}}]^-$ to $119.5(5)^\circ$ found for $[\text{Zn1}^{\text{Bu}}]^-$; all approach the 120° angle that is expected for idealized TMP geometry. The metal ion in each complex lies slightly above the trigonal plane formed by amidate nitrogens toward the vacant site ($0.19\text{--}0.14 \text{ \AA}$). The apical nitrogen N(4) is positioned perpendicular to the trigonal plane, resulting in an average $\text{N}(4)-\text{M}-\text{N}_{\text{amid}}$ angle that varies from $84.36(6)^\circ$ ($[\text{Co1}^{\text{Bu}}]^-$) to $85.96(8)^\circ$ ($[\text{Zn1}^{\text{Bu}}]^-$). The structural analysis also shows that $[\text{Co1}^{\text{Bu}}]^-$, $[\text{Ni1}^{\text{Bu}}]^-$, and $[\text{Zn1}^{\text{Bu}}]^-$ have nearly C_3 symmetry where the axis coincides with the $\text{M}-\text{N}(4)$ bond. The $\text{Ni}-\text{N}_{\text{amid}}$ and $\text{Zn(II)}-\text{N}_{\text{amid}}$ distances observed in $[\text{Ni1}^{\text{Bu}}]^-$ and $[\text{Zn1}^{\text{Bu}}]^-$ are not unusual and are similar to those reported for other amidate complexes.^{13,14,15} The average $\text{M}-\text{N}_{\text{amid}}$ bond distances in $[\text{Co1}^{\text{Bu}}]^-$ and $[\text{Ni1}^{\text{Bu}}]^-$ are statistically the same ($1.971(2)$ and $1.972(3) \text{ \AA}$) whereas in $[\text{Zn1}^{\text{Bu}}]^-$ this average distance is slightly longer at $1.986(2) \text{ \AA}$.

These structural results show that the tripodal ligand $[\text{1}^{\text{Bu}}]^{3-}$ coordinates in an identical manner to that for the metal ions in $[\text{Co1}^{\text{Bu}}]^-$, $[\text{Zn1}^{\text{Bu}}]^-$, and $[\text{Ni1}^{\text{Bu}}]^-$. An overlay of the molecular structures for the three anions is presented in Figure 2 and illustrates the structural similarities of these complexes including the nearly equivalent orientations of the appended *tert*-butyl groups. Furthermore, the potassium salts of the four complexes have nearly identical solid-state FTIR spectra which further supports their solid-state structural similarity. These spectra show the absence of amide NH vibrations and a shift of ν_{CO} bands to lower energy compared to that of $[\text{H}_3\text{1}^{\text{Bu}}]$ which is consistent with metal ion coordination through the deprotonated amidate nitrogen.

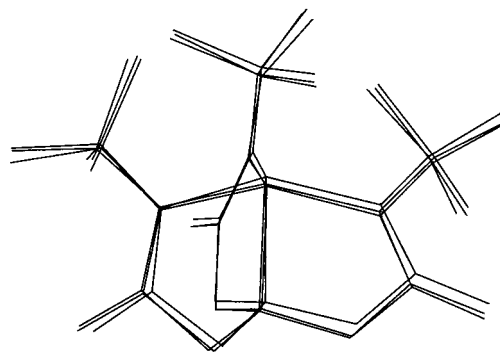


Figure 2. Overlay of the structures of $[\text{Co1}^{\text{Bu}}]^-$, $[\text{Zn1}^{\text{Bu}}]^-$, and $[\text{Ni1}^{\text{Bu}}]^-$ illustrating the similarities in their molecular structures.

Structurally characterized examples of Ni(II) and Co(II) complexes that approach a TMP coordination geometry are limited to a Ni(II) catenate^{3c} and $[\text{Co}(\text{MeTpyEA})]^{2+}$ (MeTpyEA, tris(3,5-dimethyl-1-pyrazolyethyl)amine).^{3b} Comparison of the structure of $[\text{Co1}^{\text{Bu}}]^-$ to that of $[\text{Co}(\text{MeTpyEA})]^{2+}$ shows that the Co(II) ion in $[\text{Co}(\text{MeTpyEA})]^{2+}$ is displaced toward the apical nitrogen by 0.31 \AA indicating that the structure is significantly more distorted toward a tetrahedron than observed in $[\text{Co1}^{\text{Bu}}]^-$. Similarly, the Ni(II) catenate is tetrahedrally distorted with the Ni(II) displaced by 0.33 \AA . Moreover, the only other examples of TMP Zn(II) and Fe(II) complexes are those we recently reported with related tris(*N*-alkylcarbamoyl)-methylamine ligands.^{6b,c}

Magnetic Properties. NMR studies on $[\text{Zn1}^{\text{Bu}}]^-$ support the symmetric coordination of $[\text{1}^{\text{Bu}}]^{3-}$ for this complex in solution. The ^1H NMR spectrum of the diamagnetic $[\text{Zn1}^{\text{Bu}}]^-$ in CD_3CN contains two singlet resonances at 1.34 and 2.85 ppm with an intensity ratio 9:2 that is assigned to the methylene protons of the tripodal arms and the protons of the appended *tert*-butyl groups, respectively. This result is consistent with the complex having 3-fold rotational symmetry in solution. The $[\text{Co1}^{\text{Bu}}]^-$, $[\text{Fe1}^{\text{Bu}}]^-$, and $[\text{Ni1}^{\text{Bu}}]^-$ complexes gave spectra consisting of paramagnetic shifted resonances (Experimental Section) whose assignment has yet to be determined. Room-temperature magnetic moments indicate that $[\text{Co1}^{\text{Bu}}]^-$, $[\text{Fe1}^{\text{Bu}}]^-$, and $[\text{Ni1}^{\text{Bu}}]^-$ are high-spin.¹⁶ $[\text{Ni1}^{\text{Bu}}]^-$ has a solid-state and solution effective magnetic moment of $3.49 \mu_{\text{BM}}$, which is consistent with an $S = 1$ spin system. $[\text{Fe1}^{\text{Bu}}]^-$ has a solution effective magnetic moment of $5.34 \mu_{\text{BM}}$, which is comparable to those reported for other $S = 2$ Fe(II) complexes. The solid-state effective magnetic moment of $[\text{Co1}^{\text{Bu}}]^-$ is $4.30 \mu_{\text{BM}}$, which is higher than the spin-only value of $3.87 \mu_{\text{BM}}$ for an $S = 3/2$ spin system but is similar to those reported for trigonal bipyramidal Co(II) complexes.¹⁷ In addition, powdered and solution samples of $[\text{Co1}^{\text{Bu}}]^-$ give rise to a broad X-band EPR spectrum with $g \cong 4.17$ at 77 K which further substantiates its $S = 3/2$ spin state. The high-spin character of these complexes agrees with extended Hückel calculations which show that the d_x^2 (a) orbital and the $d_{x^2-y^2}$, d_{xy} (e) set of orbitals are at nearly equivalent energies and are positioned higher than the d_{xz} , d_{yz} (e) set.

Electronic Absorption Properties. The visible electronic absorption spectra for $[\text{Co1}^{\text{Bu}}]^-$ and $[\text{Ni1}^{\text{Bu}}]^-$ are presented in Figure 3. $[\text{Zn1}^{\text{Bu}}]^-$ and $[\text{Fe1}^{\text{Bu}}]^-$ do not possess any transitions in the visible spectrum. There are few analyses of the electronic properties for TMP complexes, probably because of the dearth

(13) (a) Freeman, H. C.; Guss, J. M.; Sinclair, R. L. *J. Chem. Soc., Chem. Commun.* **1968**, 485. (b) Machida, R.; Kimura, E.; Kushi, Y. *Inorg. Chem.* **1986**, 25, 3461.

(14) Kimura, E.; Koike, T.; Iitak, Y. *Inorg. Chem.* **1990**, 29, 4621.

(15) To our knowledge, there are no reports of structural studies on complexes containing $\text{Co(II)}-\text{N}_{\text{amid}}$ bonds.

(16) Drago, R. *Physical Methods in Inorganic Chemistry*; Saunders: Philadelphia, PA, 1977; Chapter 11.

(17) Dori, Z.; Gray, H. B. *Inorg. Chem.* **1968**, 7, 889.

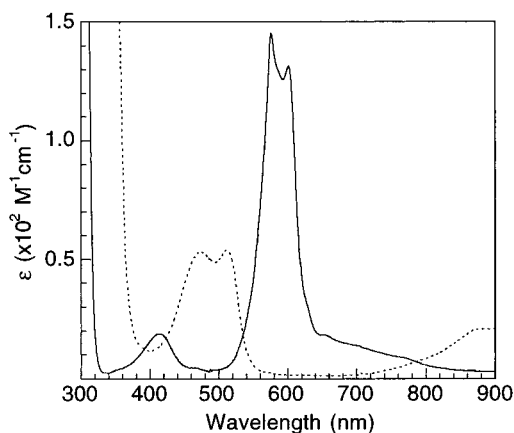


Figure 3. Electronic absorption spectra for $[\text{CoI}^{\text{Bu}}]^-$ (—) and $[\text{NiI}^{\text{Bu}}]^-$ (---) in DMF.

of structurally well-characterized examples. The only study on Co(II)–TMP complexes of which we are aware is by Gatteschi who reported an experimental and theoretical treatment of the electronic spectra of $[\text{Co}(\text{MeTPyEA})]^{2+}$.¹⁸ The solid-state diffuse reflectance spectrum of the pseudo-TMP $[\text{Co}(\text{MeTPyEA})]^{2+}$ has three absorption bands in the visible spectrum at 465, 578, and 797 nm, which have been assigned as ${}^4\text{A}_2 \rightarrow {}^4\text{A}_2$, ${}^4\text{A}_2 \rightarrow {}^4\text{E}$, and ${}^4\text{A}_2 \rightarrow {}^4\text{E}$ transitions. These assignments were made assuming C_{3v} site symmetry. For $[\text{CoI}^{\text{Bu}}]^-$, the visible absorption spectrum has three features: a symmetrical band at 414 nm, an unsymmetrical band centered at 590 nm, and a broad shoulder at 700 nm. On the basis of the similarities between the spectra of $[\text{Co}(\text{MeTPyEA})]^{2+}$ and $[\text{CoI}^{\text{Bu}}]^-$, we have tentatively assigned the bands in the spectrum of $[\text{CoI}^{\text{Bu}}]^-$ to an ${}^4\text{A}_2 \rightarrow {}^4\text{A}_2$ transition (414 nm) and ${}^4\text{A}_2 \rightarrow {}^4\text{E}$ transitions (590 and 700 nm). The higher energy observed for these transitions in $[\text{CoI}^{\text{Bu}}]^-$ compared to those found in $[\text{Co}(\text{MeTPyEA})]^{2+}$ could reflect the increased ligand field strength provided by the trigonally coordinated amidate nitrogens.

The electronic absorption spectrum for $[\text{NiI}^{\text{Bu}}]^-$ in CH_3CN also contains three features in the visible region. Two overlapping bands are found at 473 and 511 nm with molecular extinction coefficients of 49 and $51 \text{ cm}^{-1} \text{ M}^{-1}$, respectively, and a third band is observed at 877 nm ($\epsilon_{\text{M}} = 27 \text{ cm}^{-1} \text{ M}^{-1}$). Assignment of these transitions must await further analyses, but it is interesting to note that related trigonal bipyramidal complexes with C_{3v} spectroscopic site symmetry have visible absorption spectra significantly different from that found for $[\text{NiI}^{\text{Bu}}]^-$.¹⁹

Electrochemical Properties. We have investigated the redox properties of these TMP complexes by cyclic voltammetry and controlled potential coulometry. The results for the cyclic voltammetric experiments are presented in Table 3, and cyclic voltammograms (CV) for $[\text{NiI}^{\text{Bu}}]^-$, $[\text{CoI}^{\text{Bu}}]^-$, and $[\text{FeI}^{\text{Bu}}]^-$, are shown in Figure 4. The $[\text{ZnI}^{\text{Bu}}]^-$ complex did not exhibit redox processes between 1.2 and -2.0 V versus SCE. Cyclic voltammetry of the $[\text{NiI}^{\text{Bu}}]^-$ complex in MeCN between 1.8 and -2.0 V shows one quasi-reversible one-electron oxidation at $E_{1/2} = 0.56$ V vs SCE with $i_{\text{pc}}/i_{\text{pa}}^{-1} = 0.80$. Repeated scans between 1.2 and -0.40 V lead to a gradual decrease in current suggesting that the oxidized species is chemically unstable at room temperature. Moreover, at slower scan rates ($\leq 10 \text{ mV s}^{-1}$) this oxidation process becomes irreversible (Figure 4).

Table 3. Magnetic Moments^a and Electrochemical Properties^b of $[\text{NiI}^{\text{Bu}}]^-$, $[\text{CoI}^{\text{Bu}}]^-$, and $[\text{FeI}^{\text{Bu}}]^-$

complex	μ_{eff} (μ_{BM})	$E_{1/2}$ (V)	ΔE_{p} (V)	$i_{\text{c}}/i_{\text{a}}$	E_{pa} (V)
$[\text{NiI}^{\text{Bu}}]^-$	3.49	0.56 ^c	0.075 ^c	0.79 ^c	0.60 ^c
$[\text{CoI}^{\text{Bu}}]^-$	4.29	0.77	0.093	0.69	0.81
$[\text{FeI}^{\text{Bu}}]^-$	5.34 ^d		0.114	0.27	0.05

^a Solid-state. ^b In DMF at a scan rate of 0.10 V s^{-1} . ^c In MeCN. ^d In DMF.

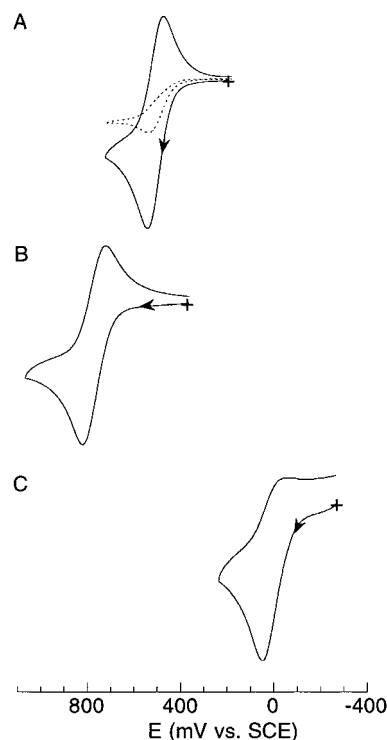


Figure 4. Cyclic voltammogram of $[\text{NiI}^{\text{Bu}}]^-$ (A), $[\text{CoI}^{\text{Bu}}]^-$ (B), and $[\text{FeI}^{\text{Bu}}]^-$ (C) recorded at a scan rate of 0.100 V s^{-1} . The dashed CV in (A) was recorded at 0.010 V s^{-1} .

Controlled-potential coulometry of $[\text{NiI}^{\text{Bu}}]^-$ at a potential of 0.70 V versus SCE produces a brown solution which has no redox processes between 1.8 and -2.0 V as gauged by cyclic voltammetry. Chemical oxidation of $[\text{NiI}^{\text{Bu}}]^-$ at room temperature produces a transient violet-colored species which rapidly changes to an EPR-silent brown material. However, chemical oxidation of $[\text{NiI}^{\text{Bu}}]^-$ at -75 °C with either $(\text{NH}_4)_2\text{Ce}(\text{NO}_3)_6$ or $[\text{Fe}(\text{bpy})_3]^{3+}$ in a 2:1 mixture of propionitrile–DMF generates a deep-violet colored solution which was stable for >48 h. As illustrated in Figure 5, at 77 K this oxidized species has a rhombic X-band EPR spectrum with $g_1 = 2.29$, $g_2 = 2.16$, $g_3 = 2.03$, and $a_3 = 20$ G. An additional small feature is observed at $g = 2.21$. This X-band spectrum is consistent with a metal-centered oxidation to form a low-spin Ni(III) species and resembles those measured for other $S = 1/2$ Ni(III) complexes.²⁰ The rhombic character of the spectrum suggests that this oxidized complex is distorted from a TMP structure which would be expected to produce a more axial spectrum. Unfortunately, repeated attempts to isolate this violet-colored oxidized Ni(III) species were unsuccessful.

The redox properties of $[\text{CoI}^{\text{Bu}}]^-$ and $[\text{FeI}^{\text{Bu}}]^-$ mirror those found for $[\text{NiI}^{\text{Bu}}]^-$. The CV of $[\text{CoI}^{\text{Bu}}]^-$ contains a quasi-reversible redox process at $E_{1/2} = 0.77$ V versus SCE at 0.100

(18) Banci, L.; Benelli, C.; Gatteschi, D.; Mani, F. *Inorg. Chem.* **1982**, *21*, 1133.

(19) Ciampolini, M. *Struct. Bonding* **1969**, *6*, 52.

(20) Salerno, J. C. In *The Bioinorganic Chemistry of Nickel*; Lancaster, J. R., Jr., Ed.; VCH: New York, 1988; Chapter 3.

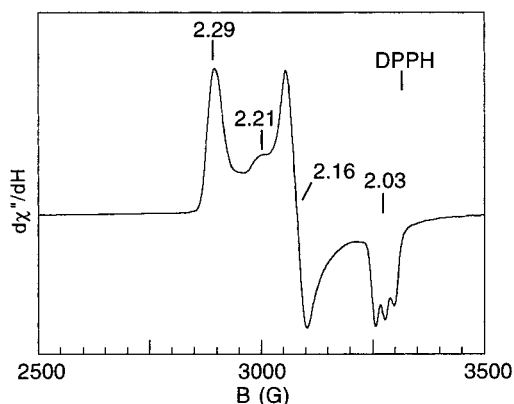


Figure 5. X-band EPR spectrum of $[\text{Ni}\mathbf{1}^{\text{Bu}}]^-$ after oxidation with $[\text{Fe}(\text{bpy})_3]^{3+}$ at -75°C measured at 77 K, 1000 G sweep width, 3000 G midrange, and 9.30 GHz, in $\text{CH}_3\text{CH}_2\text{CN}/\text{DMF}$.

V s^{-1} , yet the process becomes irreversible at slower scan rates. This redox process is assigned to the Co(III)/Co(II) couple. Chemical oxidation of $[\text{Co}\mathbf{1}^{\text{Bu}}]^-$ with $(\text{NH}_4)_2\text{Ce}(\text{NO}_3)_6$ at room temperature yielded an unstable red-colored species which is EPR silent and rapidly goes to a light brown solution. FTIR and ^1H NMR spectra of the brown solid isolated after oxidation shows the presence of $\text{H}_3\mathbf{1}^{\text{Bu}}$ as a major product. For $[\text{Fe}\mathbf{1}^{\text{Bu}}]^-$, the CV at all scan rates ($0.010\text{--}3.0\text{ V s}^{-1}$) consists of an irreversible oxidation centered at 0.050 V. Attempts to chemically or electrochemically isolate the oxidized product(s) of $[\text{Fe}\mathbf{1}^{\text{Bu}}]^-$ at room temperature yielded uncharacterized insoluble material.

Summary. We have shown in this study that the tris(*N*-alkylcarbamoyl)methylamine ligand $[\mathbf{1}^{\text{Bu}}]^{3-}$ has the correct structural properties to form trigonal monopyramidal coordination geometry around coordinatively unsaturated first-row

transition metal ions. The tris(*N*-amidate)amine chelate has enough rigidity to enforce TMP coordination while stabilizing divalent metal ions. However, the high redox potentials and lack of reversible oxidation found for $[\text{Ni}\mathbf{1}^{\text{Bu}}]^-$, $[\text{Co}\mathbf{1}^{\text{Bu}}]^-$, and $[\text{Fe}\mathbf{1}^{\text{Bu}}]^-$ suggest that this tripodal ligand cannot by itself stabilize higher oxidized metal centers. In fact, we have been unable to isolate any TMP complexes of $[\mathbf{1}^{\text{Bu}}]^{3-}$ with trivalent (or higher) metal ions even though the ligand has three diprotonated amidate moieties.^{11,12} These results contrast with those for the tripodal ligands $[(\text{XNCH}_2\text{CH}_2)_3\text{N}]^{3-}$, where TMP complexes with trivalent metal ions have been reported.⁴ One possible explanation for the inability of $[\mathbf{1}^{\text{Bu}}]^{3-}$ to stabilize high-valent metal ions is the strain that results in the chelate rings upon complexation. Several angles in the chelate rings of the divalent complexes of $[\mathbf{1}^{\text{Bu}}]^{3-}$ deviate significantly from their ideal values; for example, the $\text{C}_{\text{methylene}}\text{--C}_{\text{carbonyl}}\text{--N}_{\text{amid}}$ angle is compressed to an average value of $\sim 115^\circ$ in these complexes. Higher valent complexes would require shorter $\text{M--N}_{\text{amid}}$ bonds, and further strain within the chelate rings would result, hindering the stability of this type of chelation. This structural control of redox properties observed in complexes of $[\mathbf{1}^{\text{Bu}}]^{3-}$ is reminiscent of the entatic state found in proteins. Note that in complexes of $[(\text{XNCH}_2\text{CH}_2)_3\text{N}]^{3-}$ the chelate rings are more flexible since only one trigonal atom from the ligand is present in each ring whereas complexes of $[\mathbf{1}^{\text{Bu}}]^{3-}$ have both the trigonal amidate nitrogen and carbon atoms in their chelate rings.

Acknowledgment is made to the NIH (Grant GM50781 to A.S.B.) for financial support of this research.

Supporting Information Available: Tables of X-ray structural data for $[\text{Co}\mathbf{1}^{\text{Bu}}]^-$ and $[\text{Zn}\mathbf{1}^{\text{Bu}}]^-$ and the FTIR spectra of the complexes (Figure S1) (13 pages). Ordering information is given on any current masthead page.

IC970831E